

AN EXPERIMENTAL AND KINETIC CALCULATION OF THE PROMOTION EFFECT OF HYDROCARBONS ON THE NO–NO₂ CONVERSION IN A FLOW REACTOR

MORIO HORI,¹ NAOKI MATSUNAGA,¹ NICK MARINOV,² WILLIAM PITZ² AND CHARLES WESTBROOK²

¹*Department of Mechanical System Engineering
Takushoku University*

Hachioji, Tokyo 193, Japan

²*Lawrence Livermore National Laboratory*

P.O. Box 808

Livermore, CA 94551, USA

Experimental and detailed chemical kinetic modeling work has been performed to investigate the role of hydrocarbon oxidation in NO–NO₂ conversion. An atmospheric pressure, quartz flow reactor was used to examine the dependence of NO oxidation to NO₂ by hydrocarbon type, reaction temperature, and residence time. The five hydrocarbons examined were methane, ethylene, ethane, propene, and propane. In the experiment, probe measurement of the species concentrations was performed in the flow reactor using a mixture of NO(20 ppm)/air/hydrocarbon(50 ppm) at residence times from 0.16 to 1.46 s and temperatures from 600 to 1100 K. In the chemical kinetic calculation, the time evolution of NO, NO₂, hydrocarbons, and reaction intermediates were evaluated for a series of the hydrocarbons and the temperatures. The chemical mechanism consisted of 639 reversible reactions and 126 species.

Experimental results indicate that, in general, ethylene and propane effectively oxidize NO to NO₂ while methane is less effective. The calculation indicates the important chemical kinetic features that control NO–NO₂ conversion for each hydrocarbon type. The dependence of NO–NO₂ conversion with hydrocarbon type and temperature is qualitatively reproduced by the calculation. The calculation indicates that all five hydrocarbons oxidize NO to NO₂ predominantly through $\text{NO} + \text{HO}_2 \rightleftharpoons \text{NO}_2 + \text{OH}$ and that the contribution of oxidation by RO₂ and HORO₂ is minor. Highest effectiveness comes from hydrocarbons that produce reactive radicals (i.e., OH, O atom) that promote hydrocarbon oxidation and lead to additional HO₂ production. On the other hand, if hydrocarbons produce radicals, such as methyl and allyl, which resist oxidation by O₂, then these radicals tend to reduce NO₂ to NO. Experimental results show that the effectiveness of hydrocarbons varies appreciably with temperature and only within the low-temperature range. Propane shows the greatest NO–NO₂ conversion for the lowest temperatures. This ability is primarily due to the hydroperoxy-propyl plus O₂ reactions as indicated by the sensitivity analysis results.

Introduction

The main route to nitrogen dioxide (NO₂) formation in combustion systems is through the oxidation of nitric oxide (NO). This process was originally investigated in order to explain the high proportion of NO₂ found in NO_x emissions from the exhaust of some gas turbine engines [1]. Moreover, the understanding of the NO–NO₂ conversion mechanism is relevant to a number of issues including NO₂ emission from unflued space heaters, development of NO_x control technologies, behavior of NO/NO₂ in the atmosphere, formation and reduction chemistry of NO_x, and the probe sampling techniques for NO_x concentration measurements. Originally, the NO–NO₂ conversion was thought to proceed through the rapid oxidation of NO by oxidative radicals without much attention to the effect of fuels on the conversion [2–4]. Although, in later studies, it was revealed

that the conversion was greatly promoted by small quantities of fuels such as hydrocarbons, H₂, CO, and methanol [5–9]. In our former experiment and model calculation of the NO–NO₂ conversion in the mixing of hot combustion gas with cold air and nine different fuels [6], the results indicated that NO–NO₂ conversion appeared only in the low-temperature range and showed a strong dependence on fuel type. Thus, the interaction between the NO–NO₂ reactions and the oxidation reactions of the fuel in the low-temperature range must be understood in order to explain the effect of fuel type on the NO–NO₂ conversion and consequently to predict the NO–NO₂ emission levels from combustion systems.

The objective of the present study is to compare the experimental results obtained from a flow reactor with the calculated results of a detailed chemical model in order to understand the important controlling features of hydrocarbon oxidation kinetics on

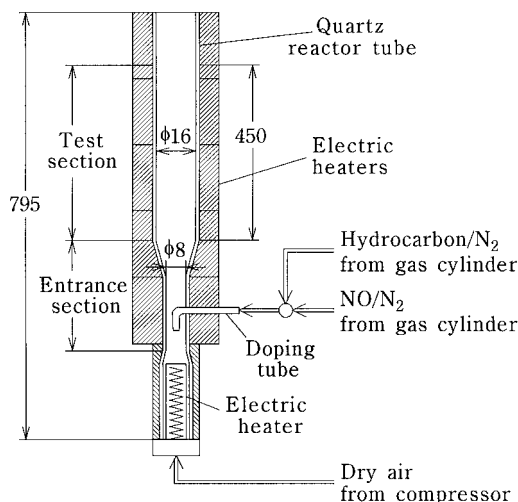


FIG. 1. Schematic of the flow reactor.

the NO–NO₂ conversion. The study is original as this effort represents a first attempt to compare the NO–NO₂ conversion dependence by hydrocarbon type and reaction temperature through a combined effort of experiment and detailed chemical kinetic modeling. Previous experiment and detailed chemical kinetic modeling studies have been conducted for methane [10,11] and ethylene [12] on NO–NO₂ conversion, and our findings confirm those previous investigations. The present study focuses on the NO–NO₂ conversion found in C₁ to C₃ hydrocarbons, that is, methane, ethylene, ethane, propene, and propane. This problem is interesting not only in the area of NO_x chemistry but also in low-temperature hydrocarbon oxidation chemistry that has been investigated extensively in studies of engine knock, cool flames, and ignition phenomena [13–15]. In the experiment, a probe measurement of species concentrations was performed in an atmospheric pressure flow reactor using a mixture of NO(20 ppm)/air/hydrocarbon (50 ppm). In the chemical kinetic calculations, the temporal evolution of NO, NO₂, hydrocarbons, and reaction intermediates for a series of hydrocarbon types and reaction temperatures is shown. The important chemical kinetic features that control the NO–NO₂ conversion for each hydrocarbon type are discussed.

Experimental

Experimental Apparatus

The experiment was performed using a constant-temperature quartz flow reactor shown schematically in Fig. 1. Dry air was supplied to an electric

heater at the bottom end of the flow reactor and the air was heated to a desired reaction temperature. Just above the electric heater, an NO–hydrocarbon (balance N₂) mixture was doped as a counterflow jet into the heated air stream. In the flow reactor, the initial NO (20 ppm)/air/hydrocarbon (50 ppm) mixture flowed up through the entrance section (mostly 8 mm i.d.) and into the test section (16 mm i.d., 450 mm length) as a reacting flow at constant temperature. The types of hydrocarbons selected were methane, ethylene, ethane, propene, and propane, and the reaction temperatures were controlled from 600 to 1100 K. Nearly uniform distribution of the species concentrations and temperature across the test section was confirmed before measurements were taken. Samples were withdrawn by a quartz sampling probe at 11 axial positions (which corresponded to residence times from 0.16 to 1.46 s) in the test section. To attain iso-kinetic sampling, the sampling probe was designed to have a larger sample inlet diameter than the diameter of the downstream sample tube. The samples were analyzed by a chemiluminescent NO–NO_x analyzer continuously and by three gas chromatographs with thermal conductivity detectors and a flame ionization detector with batch method. The species detected by the gas chromatographs were oxygen, nitrogen, hydrogen, carbon monoxide, carbon dioxide, and five hydrocarbons selected for the experiment.

Experimental Results and Discussion

According to the experimental results, the NO_x concentration remains essentially constant with residence time for all the experimental conditions investigated, and thus the decrease (increase) in the NO concentration corresponds to the increase (decrease) in the NO₂ concentration. When the hydrocarbons were not doped into the mixture, the NO₂ concentration was below 1 ppm and did not vary with residence time. From these results, it is clear that only the NO–NO₂ conversion occurs within the flow reactor and that the formation of considerable levels of NO₂ is due to the role of hydrocarbon oxidation in the NO–NO₂ conversion.

The variations of the NO–NO₂ conversion with hydrocarbon type that are shown as the NO₂/NO_x ratio against the residence time are discussed at first. At the reaction temperature of 700 K, only propane promotes the NO–NO₂ conversion as shown in Fig. 2. In this case, it was found that only propane was consumed up to 30%, which resulted in the NO₂/NO_x ratio above 0.9. At 800 K, four hydrocarbons except methane promote the NO–NO₂ conversion, while, among them, ethylene and propane effectively oxidize NO to NO₂, and ethane is less effective (see Figs. 4 and 5). Although at 1000 K, all five hydrocarbons promote the NO–NO₂ conversion, and the NO₂/NO_x ratios decrease gradually in the later

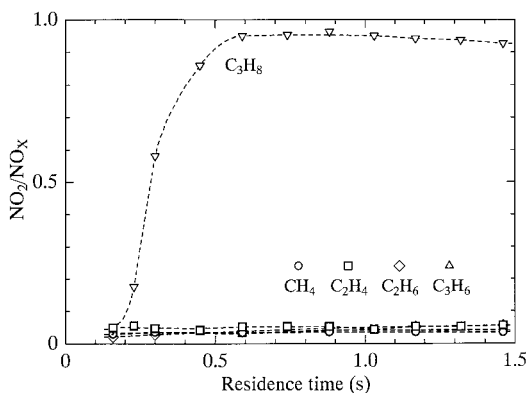


FIG. 2. NO₂/NO_x ratios against residence time obtained by the flow-reactor experiment for five hydrocarbons at 700 K.

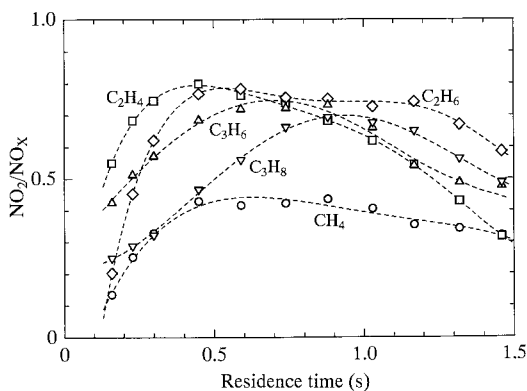


FIG. 3. NO₂/NO_x ratios against residence time obtained by the flow-reactor experiment for five hydrocarbons at 1000 K.

stage of the NO-NO₂ conversion due to the reduction of NO₂ to NO as shown in Fig. 3. In this case, it was found that the concentrations of five hydrocarbons decreased monotonically against the residence time. It is suggested from these experimental results that methane promotes the NO-NO₂ conversion most weakly and that the simple relationship is not found between the amount of hydrocarbon consumption and the level of the NO₂/NO_x ratio.

The effectiveness of hydrocarbons varies appreciably with reaction temperature and only within a low-temperature range (see Fig. 6). Propane shows the greatest NO-NO₂ conversion for the lowest temperatures, and even methane and ethane show fairly large NO-NO₂ conversion for the higher temperatures. The variations of the hydrocarbon consumption with the reaction temperature obtained in the

experiment showed that the consumption was accelerated with increasing the reaction temperature.

Chemical Kinetic Calculations

Numerical Model

The numerical calculations were performed using the CHEMKIN-II/SENKIN computer programs [16,17]. The SENKIN code was used to compute the time evolution of a homogeneous reacting gas mixture in an adiabatic system at constant pressure. The detailed chemical kinetic model used in the numerical calculations was based on a hierarchical structure of hydrocarbon oxidation kinetics starting from hydrogen and building up to propane. The main portion of the detailed kinetics mechanism was taken from our previous modeling work on hydrogen [18], methane [19], ethylene [20], ethane [19], propane [21], and ethanol [22] flame chemistry. The chemical model was extended to include NO_x chemistry and was primarily taken from GRI-MECH2.11 [23], Dean and Bozzelli [24], and Atkinson [25]. The nitrogen compounds used in the mechanism are N atom, NO, NO₂, NO₃, HNO, HONO, HONO₂, HNO₂, HNO₃, NH, NH₂, NH₃, NNH, N₂, N₂O, CN, HCN, NCO, HCNO, HNCN, HOCN, H₂CN, HCNN, CH₃NO, CH₃NO₂, CH₃ONO, CH₃ONO₂, and C₃H₅NO₂. The chemical kinetic calculations performed for propane at temperatures less than ca. 800 K by the foregoing mechanism showed no fuel conversion. A low-temperature chemistry submechanism was added to the foregoing mechanism to achieve the amount of reactivity observed in the experiments. These reactions were taken from Bozzelli and coworkers [26,27] and involve the addition of molecular oxygen to hydroperoxy-propyl radicals that eventually lead to OH radical formation and chain branching. Thermodynamic properties of the chemical compounds were obtained from the CHEMKIN Thermodynamic Database [28] or calculated by group additivity techniques as described by Benson [29] and fitted to a polynomial form using THERM [30]. The complete listing of the chemical kinetic mechanism and thermodynamics used in the modeling portion of the study can be obtained from the authors [31]. The detailed chemical kinetic model consisted of 639 reversible reactions and 126 species.

Detailed Chemical Kinetic Calculations—Results

In this section, the calculated results are compared to the experimental results. The NO₂/NO_x ratio against the residence time at 800 K is shown in Fig. 4. The experiments indicate a small amount of NO is oxidized for methane and ethane, whereas the model suggests relatively little to no conversion for

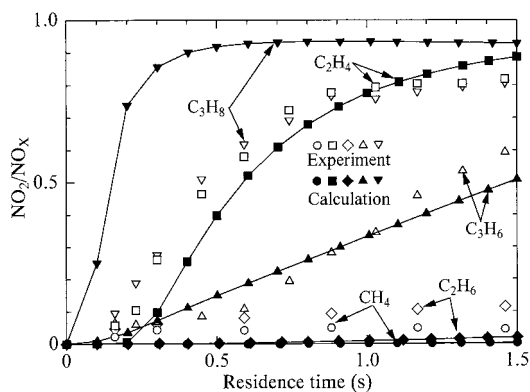


FIG. 4. Comparison between the flow-reactor experiment and the chemical kinetic calculation. NO_2/NO_x ratios against residence time for five hydrocarbons at 800 K.

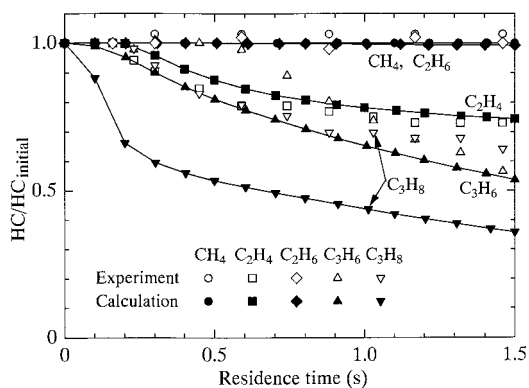


FIG. 5. Comparison between the flow-reactor experiment and the chemical kinetic calculation. Nondimensional hydrocarbon concentrations against residence time for five hydrocarbons at 800 K. (Hydrocarbon concentrations are nondimensionalized to the initial hydrocarbon concentrations.)

these fuels. The ethylene experimental data show a fairly rapid rise in NO conversion at early residence times and slowly levels out with time. The calculation shows similar behavior, although the NO_2/NO_x ratio increases a little more rapidly at longer residence times. The propene experimental data show a fairly linear increase in NO_2 formation with time that is reproduced by the model calculation. Propane exhibits nearly the same measured NO_2/NO_x profile as ethylene, although the calculation shows a greater oxidation of NO at the early residence times than indicated by the experiment. There are a number of possibilities that could account for this discrepancy. The overpredicted oxidation of NO could be due to the inadequate understanding of the propyl plus O₂ chemical activation reaction process and

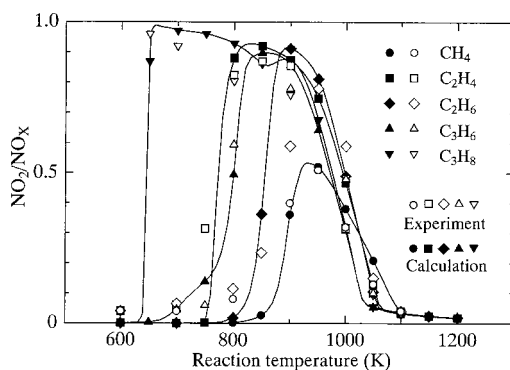


FIG. 6. Comparison between the flow-reactor experiment and the chemical kinetic calculation. NO_2/NO_x ratios at the residence time of 1.46 s against the reaction temperature for five hydrocarbons.

inaccurate thermochemical assignments to the propyl-O₂ and hydroperoxy-propyl adducts.

Figure 5 shows the hydrocarbon consumption with residence time at 800 K. The hydrocarbon concentration has been nondimensionalized to the initial hydrocarbon concentration of 50 ppm. Experimental results for methane and ethane are reproduced by the calculation and show very little hydrocarbon consumption with residence time. The experimental ethylene consumption profile is also well reproduced by the calculation. The propene experimental data show a longer induction time prior to the start of its oxidation than indicated by the calculation. At longer residence times, the propene experimental consumption profile exhibits a linear change in concentration with residence time that is a similar characteristic exhibited by the calculation. The modeling results for propane show an overoxidation of the fuel in comparison with the experimental data, and the causes for this disagreement have been previously discussed in connection to the over oxidation of NO with residence time.

The calculated change in the NO_2/NO_x ratio with temperature is compared to measurement in Fig. 6. The NO_2/NO_x ratios for five hydrocarbons are reasonably reproduced by the model. The model was able to reproduce qualitatively the low-temperature NO-NO₂ conversion behavior for propane, and the mechanism for this behavior is discussed in the next section.

Computer simulations were also performed for HO₂ and NO₂ loss within the reactor. We assumed the wall destruction of HO₂ and NO₂ as the rate-limiting case (i.e., HO₂ and NO₂ diffusion to the wall surface is fast) for HO₂ and NO₂ loss within the reactor. An HO₂ and NO₂ sticking coefficient of (no higher than) 1.0×10^{-4} and 1.0×10^{-6} , respectively, were determined as appropriate values based on these experimental measurements. Our

calculations show that these reasonable sticking coefficient values result in no loss of HO₂ and NO₂ to the reactor walls.

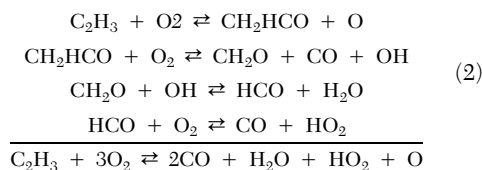
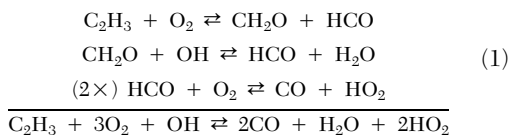
Detailed Chemical Kinetic Calculations—Analysis

Reaction flux calculations indicate that all five hydrocarbons oxidize NO to NO₂ predominantly through the NO + HO₂ ⇌ NO₂ + OH mechanism for the operating conditions examined in this study. Alkyl, alkenyl, or hydroxyalkyl plus molecular oxygen addition and subsequent stabilization of the adduct does not produce any appreciable concentration of these peroxy species that would otherwise convert the NO to NO₂ via (RO₂ or HORO₂) + NO ⇌ (RO + HORO) + NO₂. This particular NO-NO₂ conversion step was found to contribute less than 15% to NO-NO₂ conversion at the lowest temperature examined. Our numerical computations strongly suggest that the effectiveness of hydrocarbon type toward NO-NO₂ conversion depends on the hydrocarbon's propensity to produce reactive radicals like OH to sustain fuel oxidation while simultaneously producing HO₂ radicals for subsequent NO-NO₂ conversion. The production source of HO₂ is determined to occur primarily through the reaction steps of Alkyl + O₂ ⇌ Olefin + HO₂ (e.g., alkyl = *i*C₃H₇, *n*C₃H₇, C₂H₅), Alkyl-O₂ ⇌ Olefin + HO₂, HCO + O₂ ⇌ CO₂ + HO₂, and H + O₂ + M ⇌ HO₂ + M for the fuels studied at one atmosphere.

Methane does not readily promote NO-NO₂ conversion in comparison to other alkane fuels as suggested in Figs. 4 and 6. This is primarily due to the slow nature of methane oxidation that produces a limited amount of HO₂ radicals and the role of methyl radicals in reducing NO₂ via CH₃ + NO₂ ⇌ CH₃O + NO. The CH₃ radical, produced predominantly from CH₄ + OH, is difficult to oxidize by molecular oxygen as direct abstraction of H atom by O₂ is ca. 62 kcal/mol endothermic, and CH₃ + O₂ ⇌ CH₃O + O has an energy barrier of ca. 30 kcal/mol [19], thereby making this reaction enthalpically unfavorable at these temperatures. Instead, methyl radical is initially oxidized by CH₃ + O₂ ⇌ CH₂O + OH. A rate constant of 3.51 × 10¹¹ exp(-7368 K/T) cm³ mol⁻¹ s⁻¹ is used in the mechanism and is in agreement with Grella et al. [32]. This reaction initially sustains the early stages of methane oxidation and allows the HO₂ concentration to become established through the reaction steps of CH₂O + OH ⇌ HCO + H₂O, HCO + O₂ ⇌ CO + HO₂, CO + OH ⇌ CO₂ + H, and H + O₂ + M ⇌ HO₂ + M. The HO₂ reacts with NO to make NO₂ and OH, whereupon the OH is recycled back to oxidize additional methane, formaldehyde, and CO. The NO₂ can further oxidize methyl through CH₃ + NO₂ ⇌ CH₃O + NO. This reaction allows the net production of OH radical to increase via CH₃O(+M) ⇌ CH₂O + H(+M), H + O₂ + N₂

⇌ HO₂ + N₂, H + O₂ ⇌ OH + O, and NO + HO₂ ⇌ NO₂ + OH. As the temperature is raised, the amount of NO₂ formed increases as methane becomes further oxidized but is limited in conversion due to the slow HO₂ production rate and fast NO₂ reduction to NO by CH₃. The NO-to-NO₂ oxidation process then declines at the highest temperatures as H + O₂ ⇌ OH + O dominates over H + O₂ + M ⇌ HO₂ + M, thereby limiting HO₂ formation, and the additional O atom formed aids in NO₂ reduction via NO₂ + O ⇌ NO + O₂.

Ethylene readily promotes the conversion of NO to NO₂, as shown in Figs. 4 and 6, due to the main oxidation pathways producing HO₂ and reactive radicals like OH and O atom for further ethylene conversion to products. Ethylene is primarily consumed by the OH radical to make C₂H₃ and H₂O. The C₂H₃ is oxidized by two competing pathways [34], and the net reaction schemes can be expressed as:



In reaction sequence 1, two HO₂ molecules may form per ethylene consumed, thus making this pathway effective in promoting NO to NO₂. Reaction sequence 2 is an important chain-propagating pathway that sustains ethylene oxidation and indirectly allows ethylene to convert NO to NO₂ at lower temperatures than ethane. The unique synergistic effect of reaction sequences 1 and 2 in ethylene is different from the oxidation kinetics found in ethane. In ethane, the C₂H₅ + O₂ ⇌ C₂H₄ + HO₂ reaction primarily controls radical production, and HO₂ is an unreactive radical that does not contribute to the consumption of ethane via C₂H₆ + HO₂ ⇌ C₂H₅ + H₂O₂. This limits the extent of ethane consumption, thereby constraining the rate of NO-to-NO₂ conversion in the 750–850 K temperature range. These are the important chemical kinetic differences between ethylene and ethane at the low temperatures. The highest temperatures examined in the ethylene case showed the conversion of NO to NO₂ declining for the same reasons as discussed previously for the methane case.

Ethane shows a greater NO-NO₂ conversion relative to methane as indicated in Figs. 4 and 6. This is primarily due to the ease of producing HO₂ from C₂H₅ + O₂ ⇌ C₂H₄ + HO₂ and the subsequent

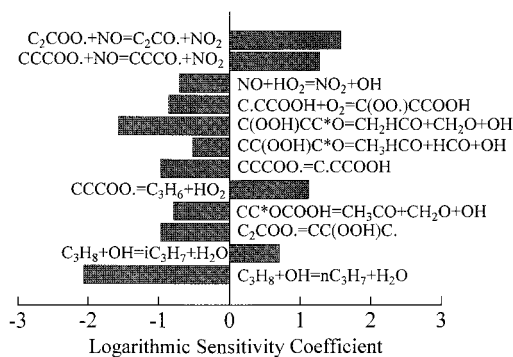


FIG. 7. Propane sensitivity analysis at 650 K. The logarithmic sensitivity coefficient determined by perturbing reaction's pre-exponential term by a factor of 1.3 and calculating the new NO value relative to the baseline, unperturbed case. A negative (positive) coefficient indicates the reaction promotes (reduces) NO–NO₂ conversion.

radical production that occurs as C₂H₄ is consumed. Ethane is primarily oxidized by OH to make C₂H₅ and H₂O. The ethyl radical reacts with O₂ and either collisionally stabilizes to the peroxy compound, C₂H₅O₂, or forms C₂H₄ + HO₂ through the chemically activated reactions of C₂H₅ + O₂ ⇌ C₂H₄ + HO₂ or C₂H₅ + O₂ ⇌ C₂H₅O₂ followed by C₂H₅O₂ ⇌ C₂H₄ + HO₂. The C₂H₅ + O₂ ⇌ C₂H₄ + HO₂ reaction exhibits an overall exothermicity of ca. 12 kcal/mol and has no energy barriers greater than the entrance channel's incoming energy. The favorable thermodynamics portrayed in C₂H₅ + O₂ ⇌ C₂H₄ + HO₂ opposed to CH₃ + O₂ ⇌ CH₂ + HO₂ allows for rapid HO₂ production in ethane oxidation while simultaneously consuming C₂H₅, thus limiting its participation in NO₂ reduction kinetics via C₂H₅ + NO₂ ⇌ CH₃CH₂O + NO. These are important differences when considering the NO–NO₂ promotion effect between ethane and methane fuels.

The NO–NO₂ conversion in propene oxidation lies between ethylene and ethane as shown in Figs. 4 and 6. The conversion is not as great as ethylene primarily due to NO₂ reduction via *a*C₃H₅ (allyl) + NO₂ ⇌ CH₂CHCH₂O + NO, yet the conversion temperature range is wider than ethane due to the greater carbon content of propene introduced into the reactive flow. Propene is initially consumed by O₂ to produce *a*C₃H₅ and HO₂. The NO + HO₂ ⇌ NO₂ + OH reaction provides the initial source of OH radicals for propene consumption. Propene is primarily removed by OH to make *a*C₃H₅ and H₂O. Allyl is a resonantly stabilized radical that is difficult to oxidize by O₂. This may be explained by noting the rate-determining energy barriers for allyl–O₂ isomerization to products typically exceeds the allyl + O₂ incoming energy by at least 12 kcal/mol [34],

and the ca. 20 kcal/mol bond strength of allyl–O₂ suggests allyl–O₂ dissociation will tend to dominate over any product formation processes. Allyl's ability to resist O₂ oxidative attack allows *a*C₃H₅ to react with NO₂ via *a*C₃H₅ + NO₂ ⇌ CH₂CHCH₂O + NO analogous to CH₃ + NO₂ ⇌ CH₃O + NO. The CH₂CHCH₂O radical produced by this NO₂ reduction step then decomposes to acrolein and H atom and makes this a reactive chain sequence. The acrolein is consumed by OH to form CH₂CHCO and CHCHCHO. The CH₂CHCO decomposes to C₂H₃ + CO, and CHCHCHO reacts with O₂ to make C₂H₂ + CO + HO₂. Acrolein is also removed by O atom to produce CH₂HCO (vinoxy) and HCO radicals. Interestingly, the acrolein oxidation sequence yields radicals typically found in ethylene oxidation [33]. The consumption of C₂H₃ and CH₂HCO by O₂ yields CH₂O, HCO, and radicals like OH, O atom, and HO₂. The reaction of C₃H₆ + OH ⇌ C₃H₆OH followed by HOC₃H₆ + O₂ ⇌ HOC₃H₆O₂ and HOC₃H₆O₂ + NO ⇌ HOC₃H₆O + NO₂ is of secondary importance to NO–NO₂ conversion. Propene reactions with O atom to form C₂H₅ + HCO or CH₃CO + CH₃ products are of minor importance in the overall propene oxidation chemistry for this study, although these reactions provide additional sources of HO₂ and CH₃ radicals.

Propane shows the greatest NO–NO₂ conversion for the lowest temperatures and widest temperature range of all five fuels studied both experimentally and computationally. The ability of propane to convert NO to NO₂ at the lower temperatures is primarily due to the hydroperoxy-propyl plus O₂ reactions that lead to the production of oxygenates and two OH radicals. The OH radicals further consume propane through C₃H₈ + OH ⇌ *i*C₃H₇ + H₂O and C₃H₈ + OH ⇌ *n*C₃H₇ + H₂O. The generated propyl radicals react with O₂, and this leads to two possible general outcomes. The reaction could produce HO₂ via chemically activated routes of *i*C₃H₇ + O₂ ⇌ C₃H₆ + HO₂ and *n*C₃H₇ + O₂ ⇌ C₃H₆ + HO₂, *i*C₃H₇ + O₂ ⇌ *i*C₃H₇O₂ followed by *i*C₃H₇O₂ ⇌ C₃H₆ + HO₂, and *n*C₃H₇ + O₂ ⇌ *n*C₃H₇O₂ followed by *n*C₃H₇O₂ ⇌ C₃H₆ + HO₂, or the reaction could form the stabilized hydroperoxy-propyl (or C₃H₆OOH) adduct. The degree of reactivity exhibited in propane is essentially controlled by the competition of chemically activated reactions producing HO₂ and olefin (i.e., C₃H₆) versus the partial equilibrium established in the C₃H₇ + O₂ ⇌ C₃H₇O₂ ⇌ C₃H₆OOH reaction sequence as determined from reaction flux analysis and suggested by the sensitivity analysis results for NO in Fig. 7. The stabilized hydroperoxy-propyl adduct readily reacts with O₂ and establishes a partial equilibrium with O₂C₃H₆OOH. The O₂C₃H₆OOH species undergoes internal H atom abstraction to make HOOC₃H₅OOH [e.g., C(OO.)CCOOH ⇌ C(OOH)CC.OOH] followed by beta-scission of the

O-O bond leading to a ketohydroperoxide [e.g., C(OOH)CC*O] and OH radical. The ketohydroperoxides primarily undergo O-O bond scission that leads to further OH radical production, chain branching, and propane consumption. The decomposition of the ketohydroperoxides increases NO-NO₂ conversion as indicated by the negative sensitivity coefficients shown for the C(OOH)CC*O \rightleftharpoons CH₂HCO + CH₂O + OH, CC(OOH)C*O \rightleftharpoons CH₃HCO + HCO + OH, and CC*OCOOH \rightleftharpoons CH₃CO + CH₂O + OH reactions. Sensitivity analysis shows hydroperoxy-propyl plus O₂ reactions, and the ketohydroperoxide decomposition reactions play an important promoting role in the NO-NO₂ conversion for propane.

The sensitivity analysis results for NO + HO₂ \rightleftharpoons NO₂ + OH showed a relatively small sensitivity coefficient in spite of its importance in promoting NO-NO₂ conversion. Reaction flux analysis indicates that this reaction dominates HO₂ consumption, and therefore, a small perturbation in the rate constant A-factor leads to a minor effect on the NO conversion. The reactions of *n*C₃H₇O₂ or *i*C₃H₇O₂ with NO exhibit larger in magnitude sensitivity coefficients than NO + HO₂ \rightleftharpoons NO₂ + OH because these reactions reduce the net production of alkylperoxy species and, in effect, indirectly limit OH and HO₂ radical production, thereby slowing the NO-to-NO₂ conversion rate as well.

Conclusions

The flow-reactor experiment indicated the following results:

1. In general, ethylene and propane effectively oxidize NO to NO₂ while methane and ethane are less effective.
2. High NO₂/NO_x ratios are obtained only within a relatively low reaction temperature range from 650 to 1000 K, though the hydrocarbon consumption is accelerated with increasing the reaction temperature. At higher reaction temperatures, the reduction of NO₂ to NO is observed at longer residence times.

The chemical kinetics modeling indicated the following results:

1. The kinetic calculation reproduces the experimental results qualitatively for the dependence of NO-NO₂ conversion with hydrocarbon type and reaction temperature.
2. Highest level of NO-NO₂ promotion comes from hydrocarbons that produce reactive radicals (i.e., OH, O atom) that further consume the parent hydrocarbon while at the same time producing HO₂ radicals for NO-NO₂ conversion via NO + HO₂ \rightleftharpoons NO₂ + OH (propane and ethylene).
3. If parent hydrocarbons (i.e., CH₄, C₃H₆) produce

daughter radicals (i.e., CH₃, *a*C₃H₅) that are resistant to oxidation by O₂, then the daughter radicals will reduce NO₂ to NO via the reaction R + NO₂ \rightleftharpoons RO + NO (R = CH₃, *a*C₃H₅). This reaction limits NO-to-NO₂ conversion. The R + NO₂ \rightleftharpoons RO + NO reaction type was found to be important in the methane and propene studies.

4. If the parent fuel can be oxidized to C₂H₄ or C₂H₃, then NO will be readily promoted to NO₂ as reactive radicals (i.e., OH, O atom) and HO₂ are produced when C₂H₃ is oxidized by O₂ (propene and ethane).

Acknowledgments

The authors would like to acknowledge the work of Yasunori Kouno and Yasunori Kawai in the experiment. The experimental and modeling work were performed respectively under the auspices of the Japan Ministry of Education (Contract Number 05650208) and the U.S. Department of Energy by the Lawrence Livermore National Laboratory (Contract Number W-7405-ENG-48).

REFERENCES

1. Cernansky, N. P., in *Progress in Astronautics and Aeronautics*, vol. 53, AIAA, 1977, p. 83.
2. Sano, T., *Combust. Sci. Technol.* 38:129-144 (1984).
3. Hori, M., in *Twenty-First Symposium (International) on Combustion*, The Combustion Institute, Pittsburgh, 1986, pp. 1181-1188.
4. Hori, M., in *Twenty-Second Symposium (International) on Combustion*, The Combustion Institute, Pittsburgh, 1988, pp. 1175-1181.
5. Bromly, J. H., Barnes, F. J., Johnston, R. C. R., and Little, L. H., *J. Inst. Energy* 58:188-196 (1985).
6. Hori, M., Matsunaga, N., Malte, P. C., and Marinov, N. M., in *Twenty-Fourth Symposium (International) on Combustion*, The Combustion Institute, Pittsburgh, 1992, pp. 909-916.
7. Bromly, J. H., Barnes, F. J., Mandyczewski, R., Edwards, T. J., and Haynes, B. S., in *Twenty-Fourth Symposium (International) on Combustion*, The Combustion Institute, Pittsburgh, 1992, pp. 899-907.
8. Nelson, P. F. and Haynes, B. S., in *Twenty-Fifth Symposium (International) on Combustion*, The Combustion Institute, Pittsburgh, 1994, pp. 1003-1010.
9. Lyon, R. K., Cole, J. A., Kramlich, J. C., and Chen, S. L., *Combust. Flame* 81:30-39 (1990).
10. Sano, T., *Combust. Sci. Technol.* 43:259-269 (1985).
11. Bromly, J. H., Barnes, F. J., Muris, S., You, X., and Haynes, B. S., *Combust. Sci. Technol.* 115:259-296 (1996).
12. Doughty, A., Barnes, F. J., Bromly, J. H., and Haynes, B. S., in *Twenty-Sixth Symposium (International) on Combustion*, The Combustion Institute, Pittsburgh, 1996, pp. 589-596.

13. Westbrook, C. K., Pitz, W. J., and Leppard, W. M., *SAE Trans.*, SAE Paper No. 91-2314.
14. Chevalier, C., Pitz, W. J., Warnatz, J., and Westbrook, C. K., in *Twenty-Fourth (International) Symposium on Combustion*, The Combustion Institute, Pittsburgh, 1992, pp. 93–101.
15. Benson, S., *Prog. Energy Combust. Sci.* 7:125–154 (1981).
16. Kee, R. J., Rupley, F. M., and Miller, J. A., *CHEMKIN-II: A Fortran Chemical Kinetics Package for the Analysis of Gas Phase Chemical Kinetics*, Sandia National Laboratories Report, SAND89-8009B UC-706, 1989.
17. Lutz, A. E., Kee, R. J., and Miller, J. A., *SENKIN: A Fortran Program for Predicting Homogeneous Gas Phase Chemical Kinetics with Sensitivity Analysis*, SANDIA National Laboratories Report, SAND87-8248 UC-401.
18. Marinov, N. M., Westbrook, C. K., and Pitz, W. J., in *Eighth (International) Symposium on Transport Processes*, vol. 1, 1995, pp. 118–129.
19. Marinov, N. M., Pitz, W. J., Westbrook, C. K., Castaldi, M. J., and Senkan, S. M., *Combust. Sci. Technol.*, 116–117:211–287 (1996).
20. Castaldi, M. J., Marinov, N. M., Melius, C. F., Huang, J., Senkan, S. M., Pitz, W. J., and Westbrook, C. K., in *Twenty-Sixth Symposium (International) on Combustion*, The Combustion Institute, Pittsburgh, 1996, pp. 693–702.
21. Marinov, N. M., Castaldi, M. J., Melius, C. F., and Tsang, W., *Combust. Sci. Technol.* 128:295–342 (1997).
22. Marinov, N. M., “A Detailed Chemical Kinetic Model for High Temperature Ethanol Oxidation,” *Int. J. Chem. Kinet.*, in press (1998).
23. Bowman, C. T., Hanson, R. K., Davidson, D. F., Gardiner Jr., W. C., Lissianski, V., Smith, G. P., Golden, D. M., Frenklach, M., and Goldenberg, M., http://www.me.berkeley.edu/gri_mech/1997.
24. Dean, A. M. and Bozzelli, J. W., in *Combustion Chemistry II*, (W. Gardiner Jr., ed.), Springer-Verlag, New York, 1997.
25. Atkinson, R., Baulch, D. L., Cox, R. A., Hampson Jr., R. F., Kerr, J. A., and Troe, J., *J. Phys. Chem. Ref. Data* 21:1125–1568 (1992).
26. Bozzelli, J. W. and Pitz, W. J., in *Twenty-Fifth Symposium (International) on Combustion*, The Combustion Institute, Pittsburgh, 1995, pp. 783–791.
27. Koert, D. N., Pitz, W. J., Bozzelli, J. W., and Cernansky, N. P., in *Twenty-Sixth Symposium (International) on Combustion*, The Combustion Institute, Pittsburgh, 1996, pp. 633–640.
28. Kee, R. J., Rupley, F. M., and Miller, J. A., *The CHEMKIN Thermodynamic Database*, Sandia National Laboratories Report, SAND86-8246, 1986.
29. Benson, S. W., *Thermochemical Kinetics*, 2nd ed., Wiley, New York, 1976.
30. Ritter, E. R. and Bozzelli, J. W., *Int. J. Chem. Kinet.* 23:767–778 (1991).
31. marinov1@llnl.gov or Marinov, N. M., LLNL Report, UCRL-JC-129372, 1998.
32. Grell, M., Amorebreta, V. T., and Colussi, A., *J. Phys. Chem.* 96:7013–7018 (1992).
33. Marinov, N. M. and Malte, P. C., *Int. J. Chem. Kinet.* 27:957–986 (1995).
34. Bozzelli, J. W. and Dean, A. M., *J. Phys. Chem.* 97:4427–4441 (1993).

COMMENTS

Anders B. Bendtsen, *Technical University of Denmark, Denmark*. You are not using the heat of formation of CH_3O_2 suggested by Bromly [1]. Do you have a comment of the effect of using a lower heat of formation for CH_3O_2 on the initial oxidation of NO through the reactions $\text{CH}_3\text{O}_2 (+ M) \rightarrow \text{CH}_3\text{O}_2 (+ M)$ and $\text{CH}_3\text{O}_2 + \text{NO} \rightarrow \text{CH}_3\text{O} + \text{NO}_2$?

REFERENCE

1. Bromly, J. H., Barnes, F. J., Muris, S., You, X., and Haynes, B. S., *Combust. Sci. Technol.* 115:259–296 (1996).

Author's Reply. Calculations were performed at 950 K for the NO (20 ppm)/air/ CH_4 (50 ppm) case by reducing the CH_3O_2 heat of formation value from Tsang's recommendation of 6.7 kcal/mol to Bromly's value of 2.7 kcal/mol (Ref. [11] in the paper). We find the change in the CH_3O_2 heat of formation value results in additional CH_3 consumption via $\text{CH}_3 + \text{O}_2 \leftrightarrow \text{CH}_3\text{O}_2$ (due to the shift in equilibrium) and a slightly greater NO-to- NO_2 conversion. The greater NO-to- NO_2 conversion is primarily due to the lower CH_3 concentration that limits the amount of NO_2 reduction to NO by $\text{CH}_3 + \text{NO}_2 \leftrightarrow \text{CH}_3\text{O} + \text{NO}$ than

the gain from $\text{CH}_3\text{O}_2 + \text{NO} \leftrightarrow \text{CH}_3\text{O} + \text{NO}_2$. The predominant NO-to- NO_2 conversion mechanism is still $\text{NO} + \text{HO}_2 \leftrightarrow \text{NO}_2 + \text{OH}$.

One additional point should be made regarding heat of formation choices. The $\text{CH}_3 + \text{O}_2$ reaction has three possible products CH_3O_2 , $\text{CH}_2\text{O} + \text{OH}$, and $\text{CH}_3\text{O} + \text{O}$. The most important products for the conditions of this study are CH_3O_2 and $\text{CH}_2\text{O} + \text{OH}$, where CH_3O_2 is intermediary to $\text{CH}_2\text{O} + \text{OH}$ from the chemical activation process of $\text{CH}_3 + \text{O}_2 \leftrightarrow \text{CH}_3\text{O}_2 \leftrightarrow \text{CH}_2\text{OOH} \leftrightarrow \text{CH}_2\text{O} + \text{OH}$. Any adjustment to the CH_3O_2 heat of formation will affect the rate-limiting $\text{CH}_3\text{O}_2 \leftrightarrow \text{CH}_2\text{OOH}$ barrier height (relative to the $\text{CH}_3 + \text{O}_2$ entrance channel energy) for $\text{CH}_3 + \text{O}_2 \leftrightarrow \text{CH}_2\text{O} + \text{OH}$. A lower heat of formation for CH_3O_2 will require a faster $\text{CH}_3 + \text{O}_2 \leftrightarrow \text{CH}_2\text{O} + \text{OH}$ rate constant. This is noted by the difference in the $\text{CH}_3 + \text{O}_2 \leftrightarrow \text{CH}_2\text{O} + \text{OH}$ rate expression assignments where Marinov has $3.51 \times 10^{11} \exp(-7368 \text{ K/T}) \text{ cm}^3/\text{mol/s}$ while Bromly has $3.31 \times 10^{11} \exp(-4500 \text{ K/T})$. The difference in activation energy nearly reflects the difference in CH_3O_2 heat of formation values used. Modeling agreement was better with our choice of CH_3O_2 heat of formation and $\text{CH}_3 + \text{O}_2 \leftrightarrow \text{CH}_2\text{O} + \text{OH}$ rate expression than Bromley's values. Additional work is required here.